Research Article Vol. 3, No. 3 / 15 March 2020 / OSA Continuum 441

OSA CONTINUUM

Measurement of the strain-optic coefficients of PMMA from 800 to 2000 nm

X. Roselló-Mechó,* M. Delgado-Pinar, A. Díez, and M. V. Andrés

Department of Applied Physics and Electromagnetism-ICMUV, University of Valencia, C/ Dr. Moliner 50, Burjassot 46100, Spain

*xavier.rosello@uv.es

Abstract: The strain-optic coefficients of PMMA are measured in a broad wavelength range from 800 to 2000 nm. The sensitivity of the azimuthal whispering gallery mode resonances to the strain is exploited to measure the strain-optic coefficients of PMMA micro-rods. The technique is based on measuring the wavelength shift of the resonances of both polarizations states, the TE and TM, when an axial strain is applied to the polymer rods. This method enables the determination of the strain-optic coefficients of the material in a broad wavelength range. In particular, in the near-infrared range, the PMMA exhibits negligible dispersion and anisotropy, and the strain-optic coefficients show constant values within the experimental error: $p_{11} = 0.298 \pm 0.010$ and $p_{12} = 0.294 \pm 0.010$.

1. Introduction

Polymer materials are widely used in photonic applications for the manufacture of polymer optical fibers (POFs) or morphology dependent polymeric resonators. A variety of polymers are used for the fabrication, being the poly(methyl methacrylate) (PMMA) one of the most employed. These PMMA structures offer several advantages over the conventional silica ones; in particular, they are of great interest as a strain sensors due to their high elastic strain limits, high fracture toughness, and high sensitivity to strain [1]. Several applications have been developed with PMMA fibers or resonators, for example: different pressure sensors based on morphology dependent resonances [2,3], thermal and strain sensors based on UV inscribed fiber Bragg gratings (FBGs) [4,5], or a strain-tunable laser based on a FBG [6]. In all these applications it is required an accurate measurement of the main optical properties of the material in order to study the performaces of the photonic devices in detail, or to design and develop new applications. Moreover, in the last decades, the number of applications based on PMMA sensors at the near-infrared range have increased [2–6], and it is necessary to determine the optical properties of the material in the whole spectral range. Although in the bibliography the refractive index value has been reported from 400 to 1400 nm [7], the values of the strain-optic coefficients are only reported at 633 nm [8], up to our knowledge. As consequence, due to the lack of measurements of these coefficients in the near-IR range, the tabulated values at 633 nm have been used throughout the whole spectral range.

In this work, we employ a measuring technique based on the excitation of the azimuthal whispering gallery modes (WGMs) to determine the individual strain-optic coefficients of PMMA micro-rods, i.e., PMMA fibers. The conventional method is based on measuring the change of the optical path of uniaxial stressed PMMA samples by using an interferometric technique [8]. Alternatively, with this new method we measure the wavelength shift of both polarizations of the WGM resonances, the TE and TM, as a function of the longitudinal strain. In the past, we used this technique to determine the strain-optic coefficients of silica fibers, and to study the variations of their optical properties under axial strain [9]. One of the main advantages of this technique is that it does not require single-mode propagation in order to characterize a given

#384509 https://doi.org/10.1364/OSAC.384509
Journal © 2020 Received 26 Nov 2019; revised 18 Dec 2019; accepted 18 Dec 2019; published 19 Feb 2020

OSA CONTINUUM

optical fiber, which is specially convenient for the case of multimode PMMA fibers. Additionally, our technique enables the characterization of the strain-optic effect, and therefore the strain-optic coefficients, at different wavelengths, using a single section of fiber. The wavelength range under study is mainly limited by the availability of light sources and the losses of the material. It is worth to note that, in this work, we characterized pure PMMA rods with no doped core. If a PMMA fiber is studied instead, the WGM based technique will provide information about the cladding material, since the resonances are surface modes located at the outer interface.

2. Theoretical description

When the Maxwell's equations are solved for an uniaxial cylindrical microresonator, the solutions of the WGMs split into two families of modes, corresponding to the polarizations TE and TM, as in the case of a isotropic microresonator [10]. The resonant wavelengths of the modes are determined by two characteristic equations:

$$\text{TE:} \quad \frac{1}{n_t}\frac{J'_m(k_0 n_t a)}{J_m(k_0 n_t a)} = \frac{1}{n_2}\frac{H_m^{(2)'}(k_0 n_2 a)}{H_m^{(2)}(k_0 n_2 a)}, \tag{1a}$$

$$\text{TM:} \quad n_z\frac{J'_m(k_0 n_z a)}{J_m(k_0 n_z a)} = n_2\frac{H_m^{(2)'}(k_0 n_2 a)}{H_m^{(2)}(k_0 n_2 a)}, \tag{1b}$$

being a the radius of the microresonator, n_t and n_z the transversal and axial components of the material refractive index tensor, n_2 the external refractive index (typically air, $n_2 = 1$), J_m and $H_m^{(2)}$ the Bessel and second class Hankel functions, respectively, being J'_m and H'_m their derivatives. The solutions of these two transcendental equations consist on a series of resonant wavelengths determined by the azimuthal and radial orders, m and l.

When an isotropic cylindrical microresonator is stretched longitudinally, the components of the refractive index tensor (n_t and n_z) suffer a perturbation that is ruled by a different combination of the strain-optic coefficients. Depending on the value of these coefficients, a uniaxial anisotropy can be generated:

$$\frac{\Delta n_t}{n_0} = -p_{et}\,\epsilon_z; \qquad p_{et} \equiv \frac{n_0^2}{2}\left[-\nu p_{11} + (1-\nu)\,p_{12}\right], \tag{2a}$$

$$\frac{\Delta n_z}{n_0} = -p_{ez}\,\epsilon_z; \qquad p_{ez} \equiv \frac{n_0^2}{2}\left[p_{11} - 2\nu p_{12}\right], \tag{2b}$$

where n_0 is the unperturbed refractive index, p_{11} and p_{12} are the individual strain-optic coefficients, ν is the Poisson's ratio, and ϵ_z is the axial strain. The coefficients p_{et} and p_{ez} are defined for simplicity. Together with the variation of the refractive index tensor, the axial strain induces a radius shrinking of the microresonator that contributes to the wavelength shift of the WGM resonances. This radius variation is given by the Poisson's ratio of the material, according to the following expression:

$$\frac{\Delta a}{a} = -\nu\epsilon_z. \tag{3}$$

By considering the variation induced by the axial strain in the refractive index and radius of the microresonator, the characteristic Eqs. (1a) and (1b) can be solved to obtain the relative shift of the WGM resonances:

$$\left[\frac{\Delta\lambda_R}{\lambda_R}\right]_{\text{TE,TM}} = \left[-\nu - \left(1 - C_{\text{TE,TM}}\right)p_{et,z}\right]\epsilon_z, \tag{4}$$

where $C_{\text{TE,TM}}$ is a small coefficient that depends on wavelength, radius of the microresonator and material refractive index [11]. The coefficient for each polarization can be determined by

OSA CONTINUUM

solving numerically the corresponding characteristic equation, Eq. (1a) or (1b), for the particular experimental parameters. By measuring the relative wavelength shift of both polarizations as a function of the strain, the strain-optic coefficients can be obtained just by solving the linear system of two equations composed by Eq. (4), by taking into account Eqs. (2a) and (2b).

3. Experimental technique

Fig. 1(a) shows a diagram of the experimental setup employed to characterize the microresonator, which consists on a rod of PMMA of $\sim 130\,\mu$m. The WGMs were excited using an auxiliary tapered silica fiber of 2 µm waist and 5 mm length. The taper was fabricated from a conventional optical fiber employing a fuse and pull technique [12]. Since the refractive indeces of the taper and resonator (PMMA) are similar, we were able to excite the WGM resonances efficiently. As it is shown in Fig. 1(b), the taper and the resonator were placed perpendicularly, and the distance between them was controlled by a piezoelectric actuator. In order to prevent possible perturbation in the coupling, both elements, taper and resonator, were in contact. At the same time, a calibrated translation stage applied a controllable axial strain to the resonator (minimum step: 0.5 µm, which corresponds to an axial strain of 3.5 $\mu\epsilon$ in our setup). The light of a set of polarized LED sources was employed to excite the resonances. The spectra of the different LED sources overlapped, allowing the characterization of the PMMA microresonator from 800 to 2000 nm, continuously without any spectral gap. An OSA was used to register the transmittance of the taper (minimum resolution of the OSA: 50 pm). The polarization of the launched light was rotated by using a polarization controller, allowing to excite either the TE or TM modes.

It is worth to point out that, for the case of our PMMA rods, the roughness of the surface was higher than in the case of silica fibers, and that the absorption coefficient was also higher. As a consequence, the Q-factor of the WGM resonances was lower than in the experiments carried out with conventional optical fibers [13]. The linewidth of a resonance in our PMMA resonators is typically ~ 60 pm. This corresponds to a Q-factor of $\sim 2.6 \cdot 10^4$. In the wavelength range studied we did not observe a significant variation of the resonances linewidth.

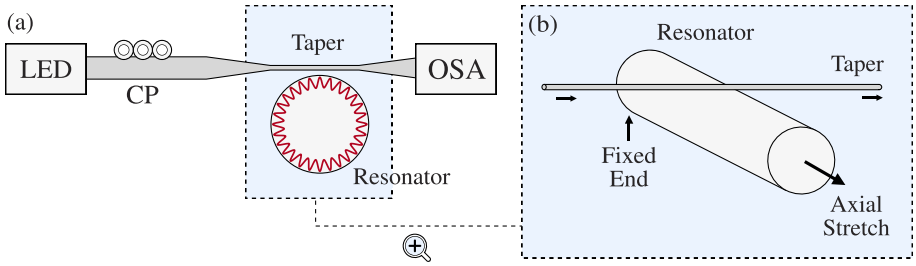

Fig. 1. (a) Scheme of the experimental setup employed to characterize the PMMA resonators. (b) Detail of the tapered fiber and the microresonator under axial strain.

Figure 2(a) shows the wavelength shift of a WGM resonance for a given axial strain of 400 $\mu\epsilon$ at ~ 1550 nm. Contrary to the case of the silica fibers, where we can observe a different response for TE and TM polarizations [9], for PMMA resonators, the TE and TM WGM resonances suffer the same shift with the strain. We observed this isotropic behavior in the whole near infrared range. As a consequence, the identification of the polarization state is not possible observing the strain response. Nevertheless, we were still able to select between each polarization, since the resonant wavelengths are not degenerated. Fig. 2(b) shows the shortest spectral distance observed between resonances of each polarization. We theoretically confirmed this by solving Eqs. (2) with the PMMA resonator parameters, and calculating the FSR and the spectral separation between modes of each polarization state.

OSA CONTINUUM

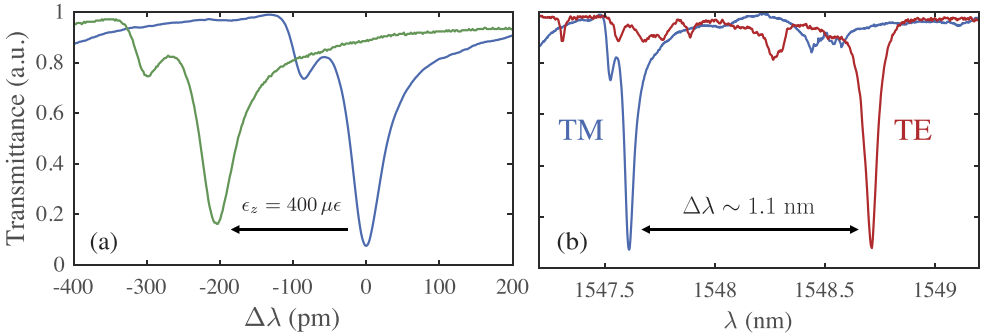

Fig. 2. (a) Illustrative example of the wavelength shift suffered by the resonances for an axial strain of $\epsilon_z = 400\,\mu\epsilon$. (b) Spectral separation between resonances of different polarization.

4. Results

Figure 3 shows the relative wavelength shift as a function of the axial strain of two WGM resonances centered at 1550 nm, one correspondent to the TE polarization and the other to the TM. Each measurement was repeated 3 times, the error in the measurements of the strain is $\pm 3.5\,\mu\epsilon$, and the error in the relative shift is obtained statistically from the 3 measurements. By fitting the experimental data we obtain the slopes of the linear regressions: $s_1 = -0.439 \pm 0.005\,\epsilon^{-1}$ and $s_2 = -0.440 \pm 0.004\,\epsilon^{-1}$. By using the method described in [14], we calculated the uncertainties of the slopes. As it can be observed, the difference between the slopes of both polarizations is within our experimental error. From the values of the slopes, the pre-calculated values of the $C_{\mathrm{TE,TM}}$ ($C_{\mathrm{TM}} = 3.115 \cdot 10^{-3}$ and $C_{\mathrm{TE}} = 4.853 \cdot 10^{-3}$, depicted in the inset of Fig. 3), and by taking into account the values of the PMMA refractive index [7], and the Poisson's ratio

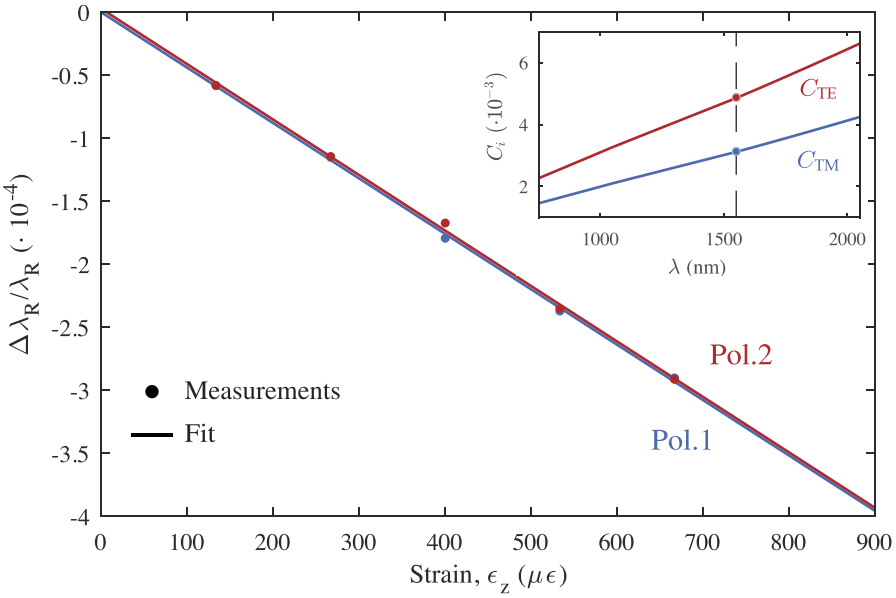

Fig. 3. Relative wavelength shift of WGM resonances as a function of the axial strain for a resonance centered at 1550 nm. *Inset*: Values of the $C_{\mathrm{TE,TM}}$ coefficients as a function of the wavelength for a PMMA rod of 130 µm of diameter.

OSA CONTINUUM

$\nu = 0.340 \pm 0.005$ [15], we can determine the strain-optic coefficients at 1550 nm. Thus, we obtained: $p_{11} = 0.283 \pm 0.021$ and $p_{12} = 0.282 \pm 0.024$.

We exploited the simplicity of the experimental technique to perform a characterization at different wavelengths: we repeated the measurements of the relative wavelength shift with the strain from 800 to 2000 nm. For all the measurements, we characterized the same PMMA rod. Following an analogous process to the case of 1550 nm, we obtained the values of the strain-optic coefficients in the whole near-infrared range. The results are depicted in Fig. 4. As the measurements show, the values of the strain-optic coefficients in the whole spectral range are constant taking into account the experimental error. Therefore, according to our results, PMMA shows a flat dispersion response and, additionally, we can point out that no anisotropy shows up. We calculated the mean value of the measurements in the whole spectral range, obtaining: $p_{11} = 0.298 \pm 0.010$ and $p_{12} = 0.294 \pm 0.010$. The uncertainty of the strain-optic coefficients is calculated from the standard deviation of the measurements. If we compare these values with the ones reported in the literature for 633 nm ($p_{11} = 0.300$ and $p_{12} = 0.297$), we can conclude that the strain-optic coefficients of PMMA does not show dispersion, neither anisotropy, from 633 to 2000 nm.

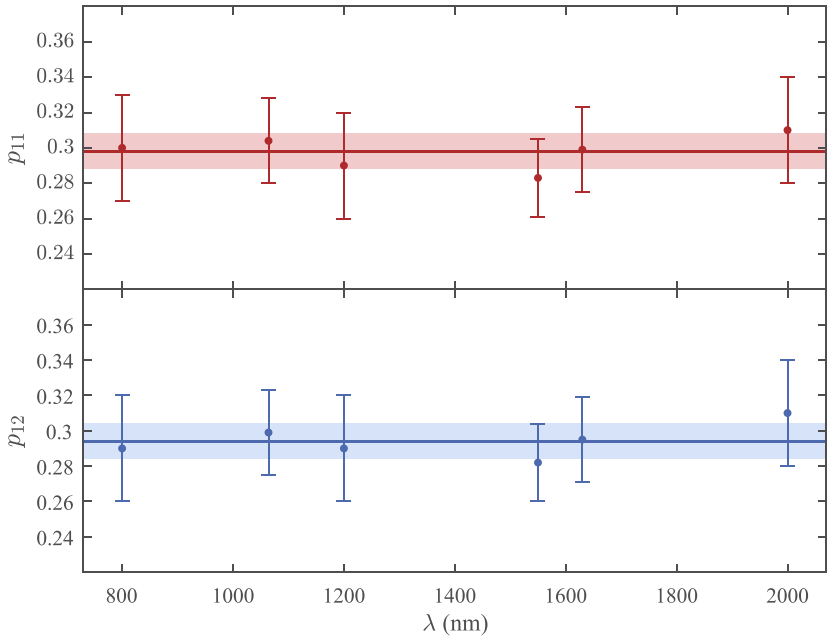

Fig. 4. Strain-optic coefficients of PMMA at different wavelengths. The solid lines indicate the mean values of the measurements in the whole spectral range. The shaded area corresponds to the standard deviation.

5. Conclusions

In conclusion, using a recently reported measuring technique, we have been able to measure the strain-optic coefficients of PMMA in a broad wavelength range, from 800 to 2000 nm. Our results show that the strain-optic coefficients of PMMA show negligible dispersion and anisotropy, and that their values in the near-infrared range 800 – 2000 nm are: $p_{11} = 0.298 \pm 0.010$ and $p_{12} = 0.294 \pm 0.010$.

OSA CONTINUUM

Funding

Agencia Estatal de Investigación (TEC2016–76664-C2-1-R); European Regional Development Fund (TEC2016–76664-C2-1-R); Conselleria d'Educació, Investigació, Cultura i Esport (PROMETEO/2019/048); Ministerio de Economía y Competitividad (BES-2014-068607).

Disclosures

The authors declare no conflicts of interest.

References

1. K. Peters, "Polymer optical fiber sensors—a review," Smart Mater. Struct. **20**(1), 013002 (2011).
2. M. A. Gouveia, P. D. Avila, T. H. R. Marques, M. C. Torres, and C. M. B. Cordeiro, "Morphology dependent polymeric capillary optical resonator hydrostatic pressure sensor," Opt. Express **23**(8), 10643–10652 (2015).
3. T. Ioppolo and M. V. Ötügen, "Pressure tuning of whispering gallery mode resonators," J. Opt. Soc. Am. B **24**(10), 2721–2726 (2007).
4. X. Chen, C. Zhang, D. J. Webb, G.-D. Peng, and K. Kalli, "Bragg grating in a polymer optical fibre for strain, bend and temperature sensing," Meas. Sci. Technol. **21**(9), 094005 (2010).
5. W. Yuan, A. Stefani, M. Bache, T. Jacobsen, B. Rose, N. Herholdt-Rasmussen, F. Kryger-Nielsen, S. Andresen, O. Brøsted-Sørensen, K. Styhr-Hansen, and O. Bang, "Improved thermal and strain performance of annealed polymer optical fiber bragg gratings," Opt. Commun. **284**(1), 176–182 (2011).
6. H. Liu, H. Liu, G. Peng, and P. Chu, "Polymer optical fibre bragg gratings based fibre laser," Opt. Commun. **266**(1), 132–135 (2006).
7. G. Beadie, M. Brindza, R. A. Flynn, A. Rosenberg, and J. S. Shirk, "Refractive index measurements of poly(methyl methacrylate) (PMMA) from 0.4-1.6 µm," Appl. Opt. **54**(31), F139–F143 (2015).
8. R. M. Waxler, D. Horowitz, and A. Feldman, "Optical and physical parameters of plexiglas 55 and lexan," Appl. Opt. **18**(1), 101–104 (1979).
9. X. Roselló-Mechó, M. Delgado-Pinar, A. Díez, and M. V. Andrés, "Measurement of pockels' coefficients and demonstration of the anisotropy of the elasto-optic effect in optical fibers under axial strain," Opt. Lett. **41**(13), 2934–2937 (2016).
10. G. Annino, M. Cassettari, I. Longo, and M. Martinelli, "Whispering gallery modes in a dielectric resonator: characterization at millimeter wavelength," IEEE Trans. Microwave Theory Tech. **45**(11), 2025–2034 (1997).
11. X. Roselló-Mechó, M. Delgado-Pinar, A. Díez, and M. Andrés, "Anisotropic elasto-optic effect in optical fibers under axial strain: a perturbative approach, in *Latin America Optics and Photonics Conference* (Optical Society of America, 2016), p. LTu4A.37.
12. J. C. Knight, G. Cheung, F. Jacques, and T. A. Birks, "Phase-matched excitation of whispering-gallery-mode resonances by a fiber taper," Opt. Lett. **22**(15), 1129–1131 (1997).
13. M. Delgado-Pinar, I. L. Villegas, A. Díez, J. L. Cruz, and M. V. Andrés, "Measurement of temperature profile induced by the optical signal in fiber bragg gratings using whispering-gallery modes," Opt. Lett. **39**(21), 6277–6280 (2014).
14. D. York, N. M. Evensen, M. López-Martínez, and J. D. Basabe-Delgado, "Unified equations for the slope, intercept, and standard errors of the best straight line," Am. J. Phys. **72**(3), 367–375 (2004).
15. M. Silva-López, A. Fender, W. Macpherson, J. Barton, J. Jones, D. Zhao, H. Dobb, D. Webb, L. Zhang, and I. Bennion, "Strain and temperature sensitivity of a single-mode polymer optical fiber," Opt. Lett. **30**(23), 3129–3131 (2005).